Fabrication and Characterization of Homogeneous Composites of Polypropylene and Multiwalled Carbon Nanotubes

Jong-Hwan Jeon, Seung-Hwa Lee, Jung-Hyurk Lim, Kyung-Min Kim

Department of Polymer Science and Engineering, Chungju National University, Chungju, Chungbuk 380-702, Korea

Received 7 March 2011; accepted 23 July 2011
DOI 10.1002/app.35340
Published online 3 November 2011 in Wiley Online Library (wileyonlinelibrary.com).

ABSTRACT: The polypropylene-grafted multiwalled carbon nanotubes (PP-MWCNTs) were produced from the reaction of PP containing the hydroxyl groups and MWCNTs having 2-bromoisobutyryl groups. The PP-MWCNTs had a significantly rougher surface than the original MWCNTs. PP-MWCNTs had PP layers of thickness 10–15 nm on the outer walls of the MWCNTs. PP/PP-MWCNT composites and PP/MWCNT composites were prepared by solution mixing in *o*-xylene. Unlike PP/MWCNT composites, PP-MWCNTs were homogeneously dispersed in the PP matrix. As a consequence, the thermal stability and conductivity of PP/PP-MWCNT composites were dramatically improved even if only 1 wt % of PP-MWNTs was added to the PP matrix. The good miscibility of PP and PP-MWCNTs plays a critical role in the formation of the homogeneous composites and leads the high thermal stability and conductivity. © 2011 Wiley Periodicals, Inc. J Appl Polym Sci 124: 3064–3073, 2012

Key words: multiwalled carbon nanotubes; polypropylene-grafted multi-walled carbon nanotubes; PP/MWCNT composite; homogeneous dispersion; solution mixing; thermal conductivity

INTRODUCTION

Carbon nanotubes (CNTs) are noted for their outstanding electrical, mechanical, and thermal properties. However, the practical uses of pristine CNTs are impeded by their aggregation properties and their insolubilities in organic solvents or water. To increase solubility and reduce the tendency of aggregation, CNTs are often functionalized with organic moieties and polymers.[1–5]

Polyolefins (polypropylene or polyethylene) constitute the family of the most influential and versatile polymers of commercial importance due to their attractive properties and low cost.[6,7] The continuous development for polyolefin-based materials aims at obtaining new enhanced properties for achieving further expansion toward new application areas. Great expectations are presently connected with the enhancement of polymer properties by employing CNTs as reinforcement filler for obtaining novel multifunctional composites combining improved mechanical and thermal properties, electric conductivity, and reduced flammability at low CNT contents.[8–10] Recent advances in CNT synthesis have enabled their large-scale production with low commercial prices comparable to conventional carbon fibers,[11] which open up the possibility for the mass production of composites. However, despite excellent properties of polymer/CNT composites as aforementioned, the poor solubility and self-aggregation of CNTs by van der waals forces disturb the improved properties of polymer/CNT composites, which have been still remaining as a challenge for both academia and industry.[12] Therefore, the major issue for preparing the polymer/CNT composites is how to maximize the interfacial compatibility between CNTs and the polymer matrix.

Many research groups have focused on the functionalization of CNTs with various organic, inorganic, and organometallic structures using both noncovalent and convalent approaches.[13] Noncovalent interactions such as π–π interactions, π–cation interactions, and ionic interactions between CNTs and polymers enable the attachment of polymers onto the surfaces of CNTs.[14–18] The covalent functionalization of CNTs with polymers includes effective both "grafting-from" and "grafting-to" approaches. For the "grafting-from" method, polymers are *in situ* grown from CNTs commonly using surface-initiated polymerization such as atom transfer radical polymerization[19–26] and reversible addition-fragmentation chain transfer polymerization.[27,28] For the "grafting-to" method, preformed polymers are grafted to CNTs through special reactions such as esterification and

Correspondence to: K.-M. Kim (kmkim@chungju.ac.kr).
Contract grant sponsor: Basic Science Research Program through the National Research Foundation of Korea (NRF), Ministry of Education, Science and Technology; contract grant number: 2010-0016092.
Contract grant sponsor: University Sabbatical Program of Chungju National University.

amidization between suitable functional groups of CNTs and polymers.[29–32]

Polypropylene/CNT composites have previously been prepared by melt processing with CNT concentration ranging from 5 to 20% to the polypropylene. This approach is the simplest method to fabricate polypropylene/CNT composites without any modification of the surface of CNTs. However, it usually results in the unfavorable effect on improvement in thermal and electrical properties of the polypropylene/CNT composites even with high CNTs concentration because of the low compatibility between CNTs and polymer.

With this in mind, we already reported the new polystyrene/polystyrene-grafted MWCNT composites by the solution mixing and found that PS-MWCNTs were homogeneously dispersed in the PS matrix because PS and PS-MWCNTs were favorably interacted.[33] This concept can be applied to polypropylene/CNT composites using the high compatibility of PP and PP-MWCNTs.

In this study, we first synthesized PP-MWCNTs by the reaction of PP containing the hydroxyl groups (PP-OH) and MWCNTs having 2-bromoisobutyryl groups (MWCNT-Br) via the "grafting to" method. MWCNT-Br was synthesized by the reaction of 2-bromoisobutyryl bromide (BiBB) and hydroxyl groups of MWCNT-OH in toluene at 105°C using triethylamine as a catalyst. Polypropylene-graft-maleic anhydride (PP-MAH) was reacted with ethanolamine to produce PP-OH. From the scanning electron microscopy (SEM) and transmission electron microscopy (TEM) images, PP-MWCNTs had a significantly rougher surface than the original MWCNTs. PP-MWCNTs had PP layers of thickness 10–15 nm on the outer walls of the MWCNTs. For our final goal to make homogeneous PP/PP-MWCNT composites with high thermal conductivity and thermal stability, PP/PP-MWCNT composites were prepared by solution mixing in *o*-xylene at 150°C. For PP/MWCNT composites prepared by PP and MWCNTs, several aggregated masses of MWCNTs are easily observed in the PP matrix, whereas PP-MWCNTs are spatially well-dispersed in the PP matrix through the good compatibility between PP and PP-MWCNTs, as evidenced by photograph images and SEM images of cryogenically fractured surface. Moreover, the thermal stability and thermal conductivity of PP/PP-MWCNT composites were dramatically improved even if only 1 wt % of PP-MWCNTs was added to the PP matrix as compared to those of PP/MWCNT composites and the pure PP.

EXPERIMENTAL

Materials

MWCNTs were obtained from the Iljin Nanotech. (diameter: 10–20 nm, length: 10–50 μm, >90 vol % of purity). Polycarbonate membrane (pore size: 200 nm) was obtained from the Whatman International. PP-MAH was purchased from Aldrich (maleic anhydride: 8–10 wt %, average M_n: 3900, average M_w: 9100). BiBB was purchased from Aldrich and used without further purification. Triethylamine were distilled over calcium hydride. Hydrogen peroxide (H_2O_2) (30%), nitric acid (HNO_3) (60%), and all solvents were obtained from Aldrich.

Characterization

Fourier transform infrared (FTIR) spectra were recorded on a FTS-6000 (BIO-RAD) spectrometer. The thermal behavior was examined with thermogravimetric analysis (TGA) (TGA S-1000, SCINCO) under nitrogen atmospheres. Raman spectrophotometer (NRS-3200, JASCO) were used to confirm and characterize PP-MWCNTs which was formed after the modification of MWCNTs. The morphologies and structures of PP-MWCNTs were observed by SEM (JSM-6700, JEOL) and energy filtering transmission electron microscope (EF-TEM) (Libra 120, ZEISS). For EF-TEM observation, the sample of PP-MWCNTs was prepared by redispersing in toluene and the solution was dropped onto a carbon-coated copper grid and then dried under vacuum. The dispersions of MWCNTs and PP-MWCNTs in the PP matrix were measured by using the camera (D40, NIKON). The thermal diffusivity and density of PP/PP-MWCNT composites were examined with thermal diffusivity system (TC-7000, ULVAC-RICO) and electronic densimeter (MD-300S, ALFAMIRAGE). The actual heat capacity were measured by differential scanning calorimetry (DSC) (DSC N-650, SCINCO) in an inert atmosphere at a heating rate of 10°C/min.

Preparation of MWCNTs containing 2-bromoisobutyryl group (MWCNT-Br)

Typically, 6.0 g of crude MWCNTs and 200 mL of 30% H_2O_2 were added into a 500 mL flask equipped with a condenser under vigorous stirring. The flask was immersed in a sonication bath (40 kHz) for 2 h. The mixture was then stirred at 90°C for 24 h. After cooling to room temperature, the reaction mixture was diluted with 800 mL of deionized water and then vacuum-filtered through a 0.2 μm polycarbonate filter paper. The dispersion, filtering, and washing steps were repeated until the pH of the filtrate was reached to 7. The filtered solids were washed with about 100 mL of acetone and THF at five times to remove the water from the sample and dried under vacuum for 24 h at 60°C. The obtained MWCNT-OH (3.0 g) and toluene (200 mL) were introduced a 300 mL flask, and the mixture was sonicated for 2 h. Then, BiBB)(6.7 mL, 54.4 mmol)

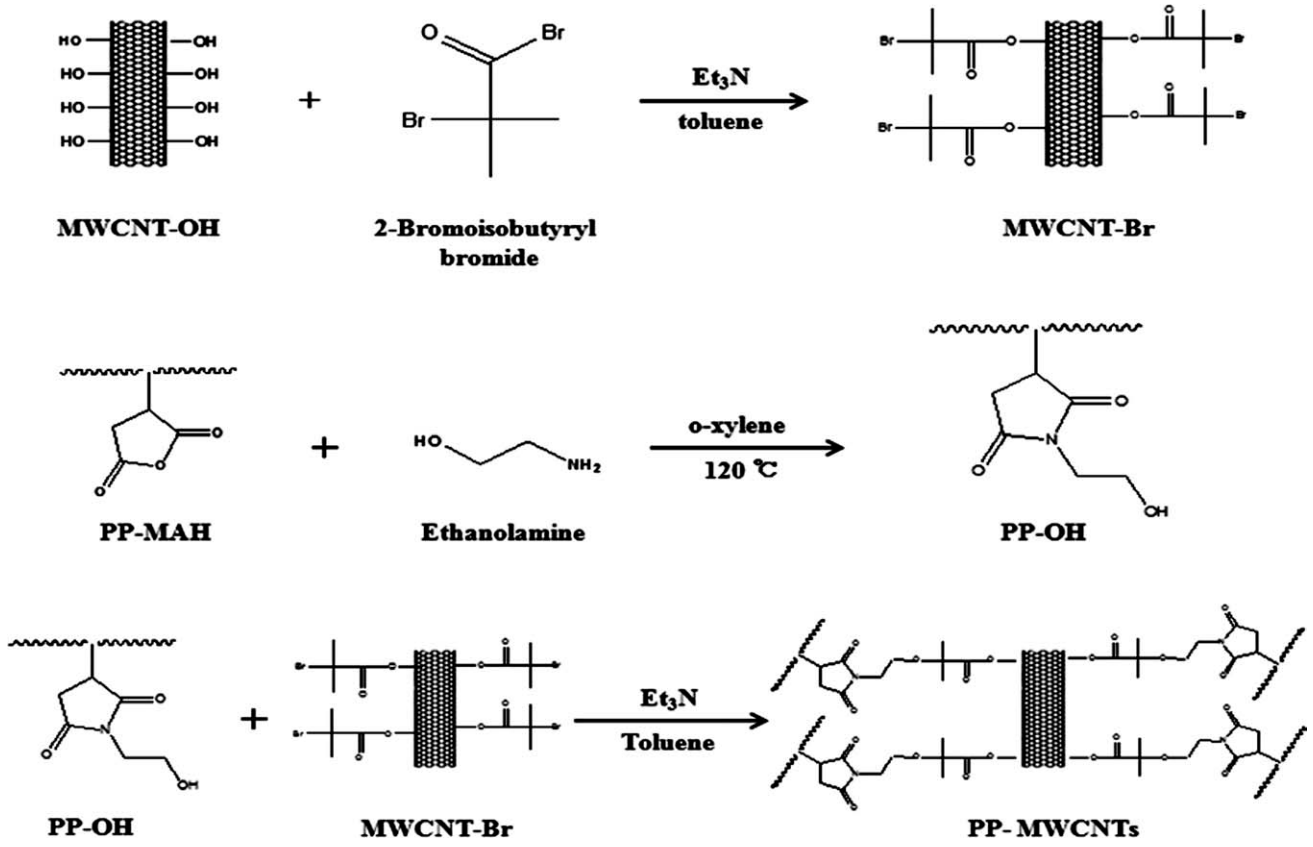

Scheme 1 Synthesis of PP-MWCNTs.

and triethylamine (8.1 mL, 54.4 mmol) were charged. After stirring 2 h at room temperature to form a black suspension, the flask was fitted with a condenser and the mixture was stirred at 105°C for 24 h under nitrogen. The reaction mixture was collected by filtration, washed with methanol, and dried in vacuum at 80°C for 12 h.

Preparation of PP containing hydroxyl groups (PP-OH)

A typical process is as follows: 700 mL of *o*-xylene and PP-MAH (75 g, 2.5 mmol-MAH) were placed in a 1 L glass reactor equipped with a mechanical stirrer and reacted at 120°C for 3 h under a nitrogen atmosphere. Then, ethanolamine (200 mL, 3.3 mmol) was added and the mixture was maintained at 120°C for 6 h under stirring. The reaction mixture was poured into 2 L of acetone. The precipitated polymer was collected by filtration, washed with acetone, and dried in vacuum at 80°C for 10 h to give 75.1 g of PP-OH as a white powder.[34]

Synthesis of PP-MWCNTs

MWCNT-Br (0.5 g) and 150 mL of toluene were introduced into a 250 mL flask and the mixture was sonicated for 3 h. Then, PP-OH (5.0 g) and triethylamine (8.1 mL, 54.4 mmol) were charged. After stirring 2 h at room temperature to form a black suspension, the flask was fitted with a condenser and the mixture was stirred at 120°C for 72 h under nitrogen. The mixture was collected by filtration, washed thoroughly with hot toluene, and the modified MWCNTs were dried under vacuum overnight.

Fabrication of PP/PP-MWCNT composites

PP/PP-MWCNT composites were prepared by solution mixing in *o*-xylene. PP- MWCNTs (0.1 g) and 200 mL of *o*-xylene were added into a 300 mL flask and sonicated for 3 h at room temperature to obtain the homogeneous solution. Ten gram of PP was added into the solution and the mixture was stirred at 150°C for 2 h. The mixture was poured into 1 L of methanol. The precipitate was filtered though a 200 nm pore membrane and dried under vacuum. (PP/MWCNT composites were prepared by same procedures used for PP/PP-MCWNT composites).

RESULTS AND DISCUSSION

The synthesis scheme of PP-MWCNTs is shown in Scheme 1. MWCNT-OH was synthesized by the MWCNTs under the hydrogen peroxide solution at 90°C. MWCNT-OH was reacted with BiBB to

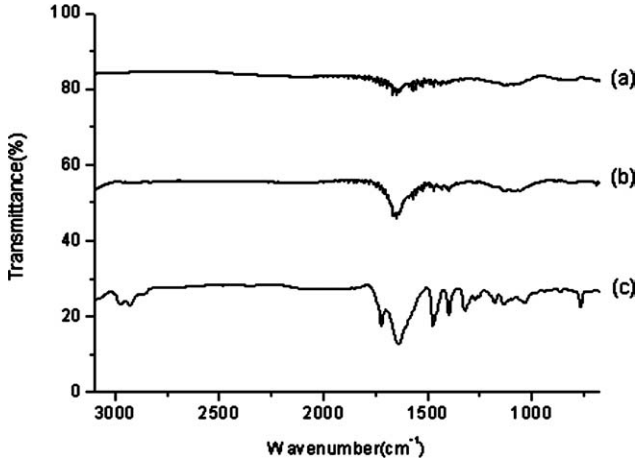

Figure 1 FTIR spectra of (a) MWCNTs, (b) MWCNT-OH, and (c) MWCNT-Br with KBr.

produce MWCNT-Br. In general, the bromination reaction is preferably performed under mild conditions to avoid any side reactions. However, in the case of this reaction containing CNTs, high temperature and long reaction time are often needed to complete the reaction owing to low solubility and low hydroxyl group concentration. Therefore, the reaction was carried out in toluene solution at 105°C for 24 h through the addition of an excess amount of BiBB and triethylamine. To make PP-OH, PP-MAH was reacted with ethanolamine in the xylene solution at 120°C for 3 h. Finally, we fabricated PP-MWCNTs by the reaction of MWCNT-Br and PP-OH under the triethylamine as a catalyst.

Figure 1 presents the FTIR spectra of (a) MWCNTs, (b) MWCNT-OH, and (c) MWCNT-Br. The spectrum of MWCNTs shows a weak absorption peak at 1632 cm^{-1}, which is related to the C=C stretching vibration of MWCNT backbones. The spectrum of MWCNT-OH shows C—O stretching peak of hydroxyl group between 1260 and 1000 cm^{-1}. After the reaction of MWCNT-OH and BiBB, new absorption peaks for ester group in the region of 1710 cm^{-1} (C=O stretch) and 1300–1160 cm^{-1} (C—O stretch) were occurred as a result of the attachment of 2-bromo-2-methylpropionate group onto the surfaces of the MWCNTs.

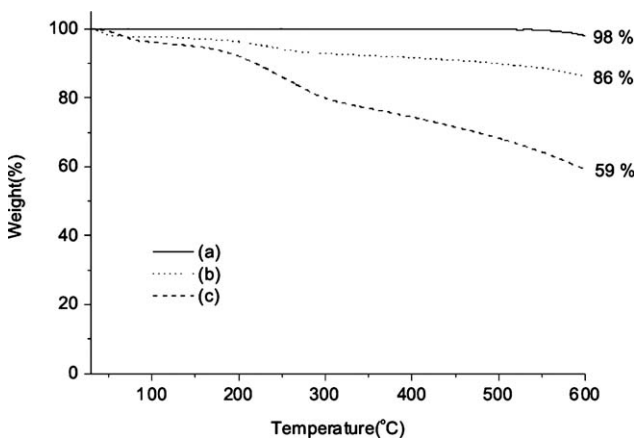

Figure 2 TGA thermograms of (a) MWCNTs, (b) MWCNT-OH, and (c) MWCNT-Br with a heating rate of 10°C/min under nitrogen atmosphere.

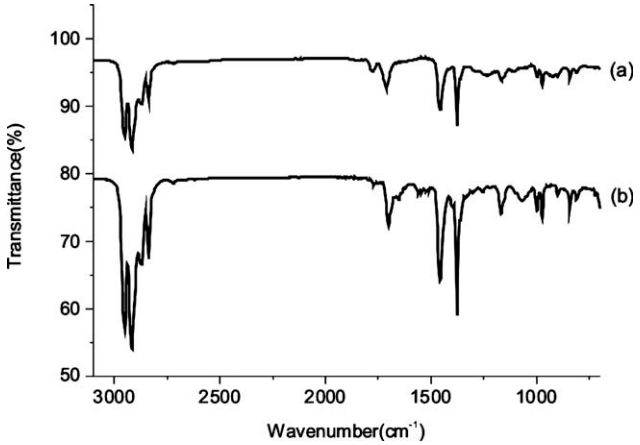

Figure 3 FTIR spectra of (a) PP-MAH and (b) PP-OH with KBr.

Figure 2 shows TGA traces of (a) MWCNTs, (b) MWCNT-OH, and (c) MWCNT-Br in an inert atmosphere at a heating rate of 10°C/min. Clearly, MWCNTs have good thermal stability. When the temperature is increased up to 600°C, there is no obvious decomposition in the MWCNTs. The residual content of the MWCNTs was 98% as shown in Figure 2(a). Figure 2(b,c) show the difference from the weight of the residue between MWCNT-OH (ca. 86%) and MWCNT-Br (ca. 59%). This can be attributed to the attachment of 2-bromoisobtyryl bromide on to the surfaces of MWCNT-OH.

Figure 3 presents the FTIR spectra of (a) PP-MAH and (b) PP-OH. The spectrum of PP-MAH shows the absorption bands at 1780 and 1632 cm^{-1}, which

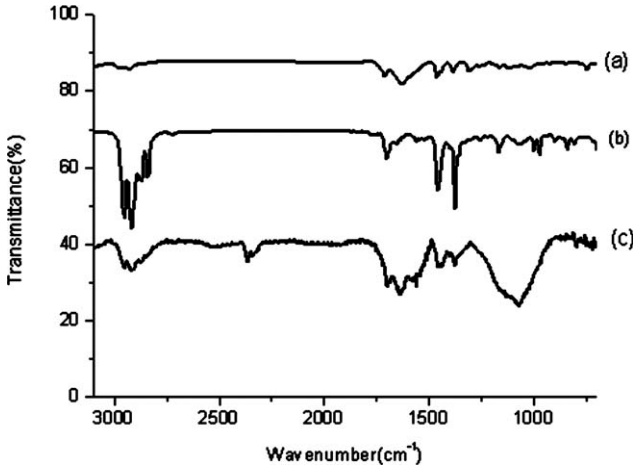

Figure 4 FTIR spectra of (a) MWCNT-Br, (b) PP-OH, and (c) PP-MWCNTs with KBr.

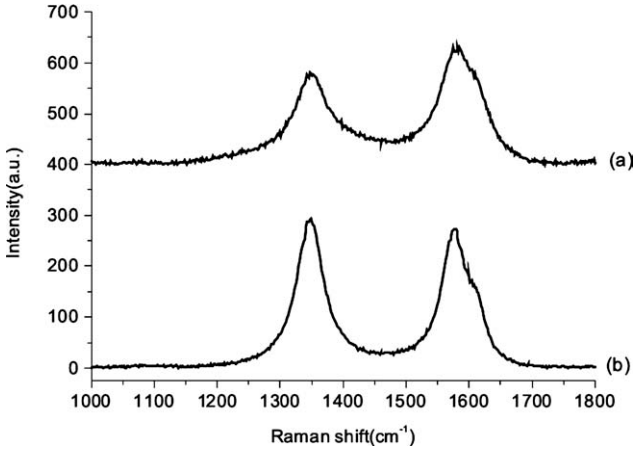

Figure 5 Raman spectra of (a) MWCNTs and (b) PP-MWCNTs.

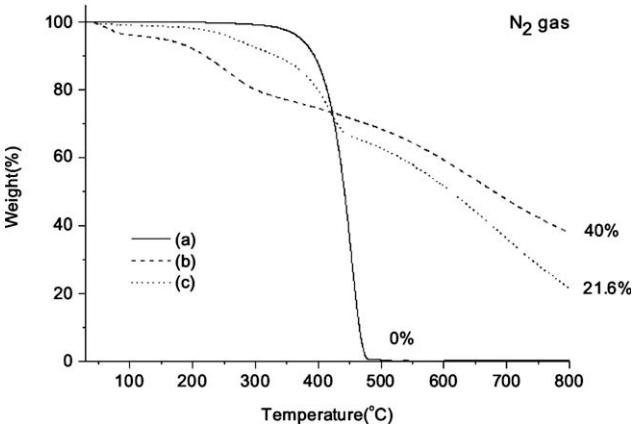

Figure 6 TGA thermograms of (a) PP-OH, (b) MWCNT-Br, and (c) PP-MWCNTs with a heating rate of 10°C/min under nitrogen atmosphere.

is related to the C=O stretching vibration of the succinic anhydride group. After the reaction with ethanolamine, the absorption bands for C—O stretching vibration around 1700 cm^{-1} was appeared as shown in Figure 3(b).

These absorption bands might be assigned to a succinimide group, suggesting that succinic anhydride group was predominantly reacted with amino group rather than hydroxyl group of ethanolamine.

Figure 4 presents the FTIR spectra of (a) MWCNT-Br, (b) PP-OH, and (c) PP-MWCNTs. The spectrum of MWCNT-Br shows a weak absorption peak at 1710 and 1300–1160 cm^{-1}, which is related to the C=O and C—O stretching vibration of ester group of 2-bromo-2-methylpropionate onto the surfaces of MWCNTs. The spectrum of PP-OH shows sp^3 C—H stretching peak of the PP backbones around 2900 cm^{-1} and C=O stretching vibration of the succinimide group at 1700 cm^{-1}. After the surface modification of MWCNTs in PP-MWCNTs, new absorption peak for PP backbone in the region of 2950–2800 cm^{-1} was occurred as a result of the incorporation of

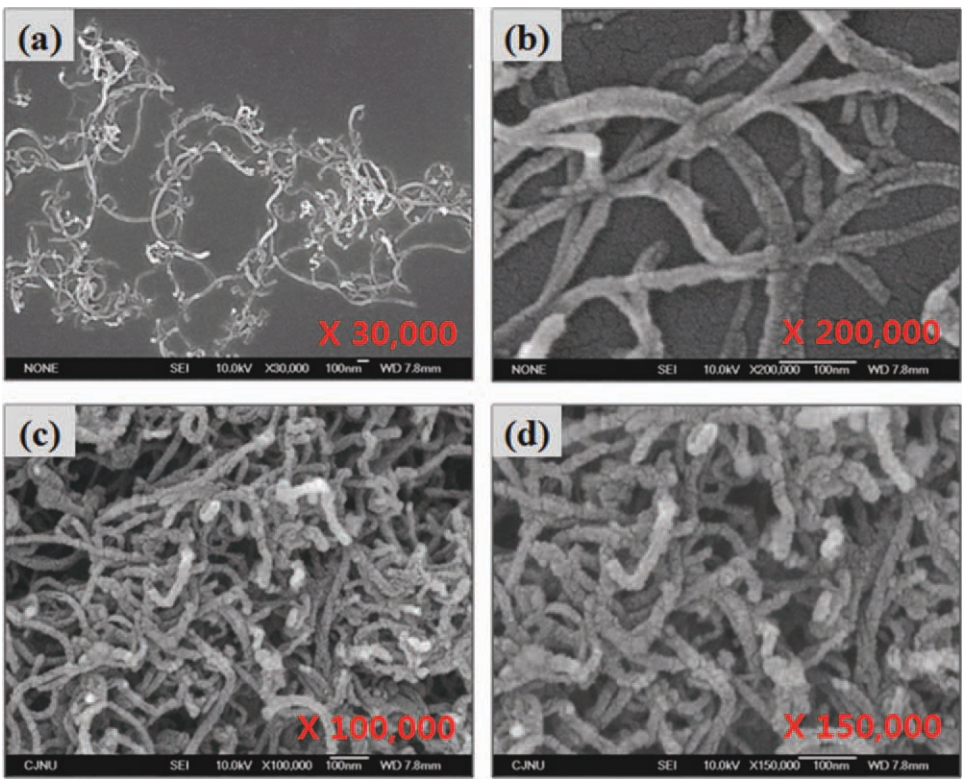

Figure 7 FE-SEM images of (a,b) MWCNTs and (c,d) PP-MWCNTs on Si-wafer. [Color figure can be viewed in the online issue, which is available at wileyonlinelibrary.com.].

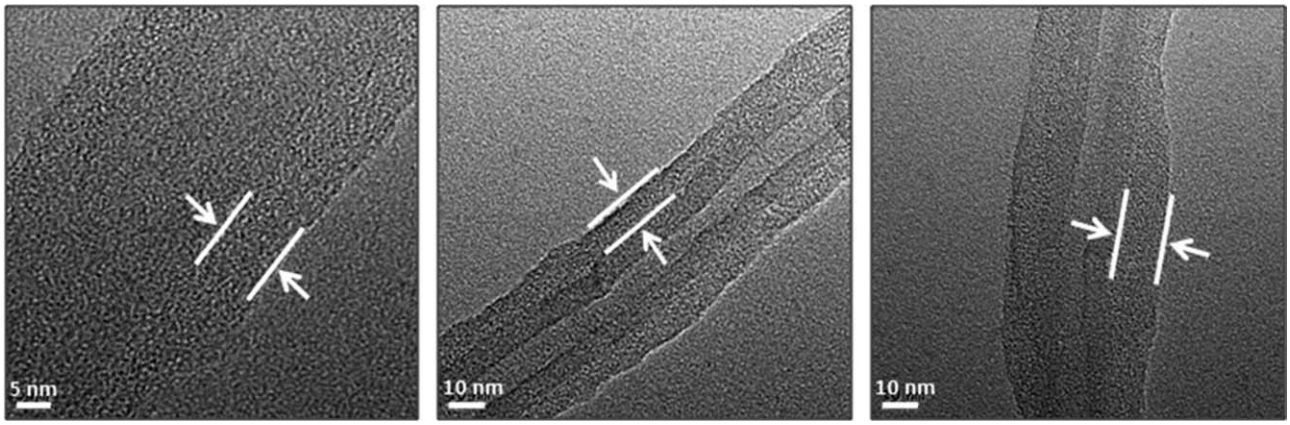

Figure 8 TEM images of PP-MWCNTs on carbon-coated copper grid.

grafted PP onto the surfaces of MWCNTs. As shown in Figure 4(c), for PP-MWCNTs, three peaks were appeared at 1700, 1450, and 1376 cm^{-1}.

Raman spectroscopy provides qualitative information about the polymer-modified MWCNTs. Raman spectra of the MWCNTs and PP-MWCNTs display two obvious peaks as shown in Figure 5. This shows characteristic G-mode or the tangential mode peaks at 1580 cm^{-1} and a disorder transition D band peaks at 1345 cm^{-1} for the MWCNTs and PP-MWCNTs, respectively. In general, the intensity of the D band is used to probe the degree of modification. Figure 5(b) shows that the intensity enhancement of D band in PP-MWCNTs proves the covalent bonding of PP onto the MWCNTs. The ratio of the intensity of the disordered (D band) to the ordered (G band) transition, which indicates the generation of surface defects due to modification, increases from 0.92 (MWCNTs) to 1.07 (PP-MWCNTs).

The thermal stability of PP-OH, MWCNT-Br, and PP-MWCNTs was observed by TGA thermograms in an inert atmosphere at a heating rate of 10°C/min as shown in Figure 6. The PP-OH was completely decomposed in the temperature range between 370 and 502°C. When the temperature was increased up to 800°C, the residual content of MWCNT-Br was 40%. Figure 6(b,c) show the difference from the weight of the residue between MWCNT-Br (ca. 40 wt %) and PP-MWCNTs (ca. 21.6 wt %). This result suggests that PP chains are well-deposited on the surface of the MWCNTs through the reaction of PP-OH and MWCNT-Br.

As described earlier, all the characterizations effectively demonstrate that the well-defined PP chains

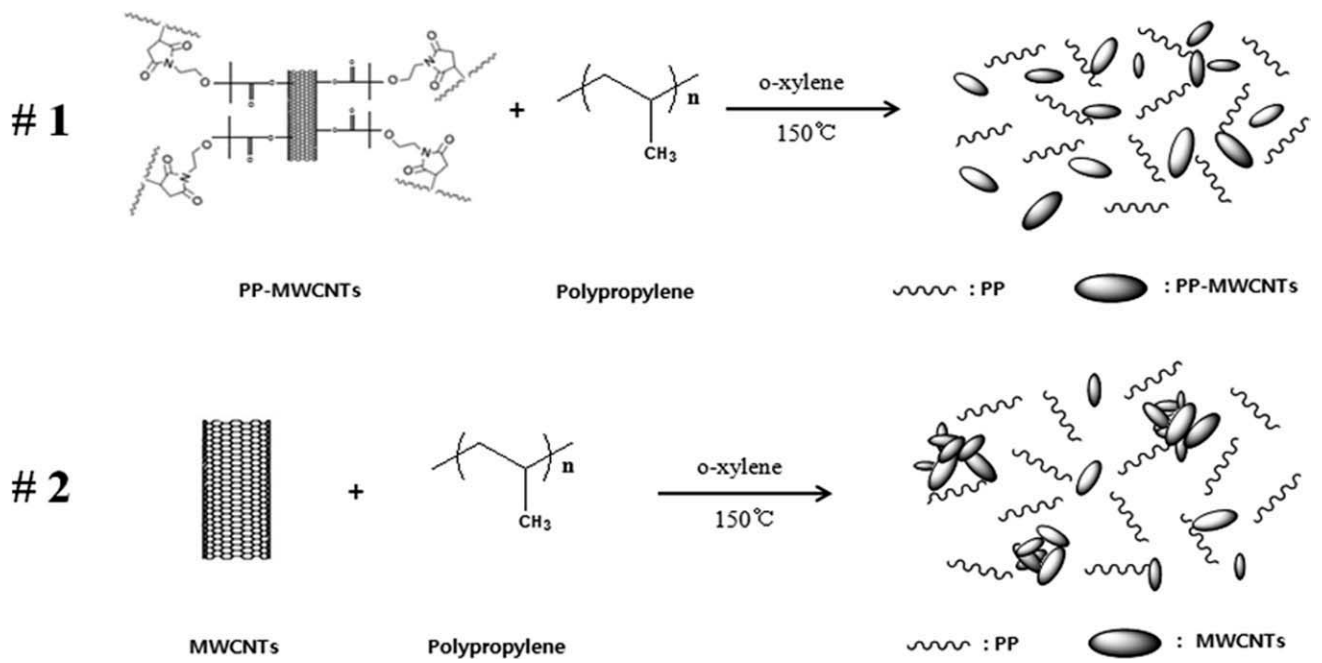

Scheme 2 Fabrication of PP/PP-MWCNT composites and PP/MWCNT composites by solution mixing.

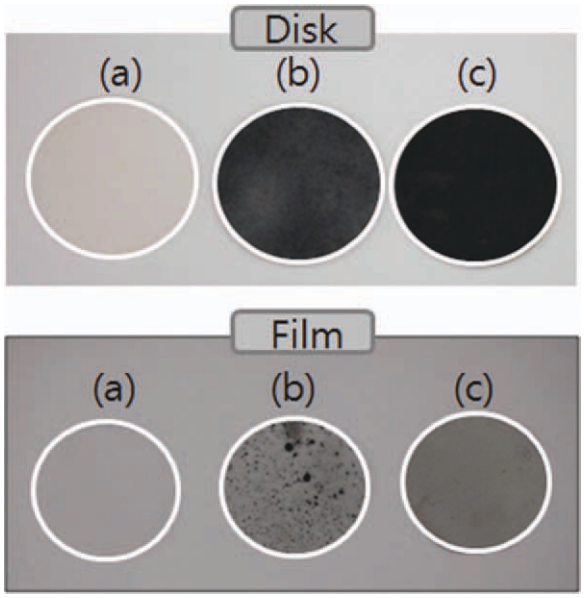

Figure 9 Photograph images of (a) PP, (b) PP/MWCNT composites, and (c) PP/PP-MWCNT composites.

are covalently grafted onto the MWCNTs with high loading efficiency. Measurements of SEM images can provide further direct evidence for PP-MWCNTs. SEM images of the MWCNTs and PP-MWCNTs are shown in Figure 7. Figure 7(a,b) present typical SEM images of the MWCNTs, showing a very clean surface for all the MWCNTs. However, the functionalization of MWCNTs with the PP changes the roughness of the MWCNTs surface, which means that PP-MWNTs have a significantly rougher surface than the original MWCNTs. In addition, irregular structures observed on the MWCNT surfaces reveal that the functionalization takes place in spherical shapes on the MWCNT surfaces as shown in Figure 7(c,d).

For TEM observation, the sample of PP-MWCNTs was prepared by redispersing in toluene and the solution was dropped onto a carbon-coated copper grid and then dried under vacuum. Direct structural characterization of individual PP-MWCNTs was realized by FE-TEM and PP-MWCNTs images were presented in Figure 8. PP-MWCNTs have PP layers of thickness 10–15 nm on the outer walls of the MWCNTs. This result confirms that PP is homogeneously deposited onto the surface of the MWCNTs.

In general, MWCNTs can easily aggregate each other due to the high surface area and van der Waals attraction, which still causes the immiscibility with organic polymers. To overcome this disadvantage, we have produced the homogeneous composites of PP and PP-MWCNTs through the high miscibility of PP and PP-MWCNTs (Scheme 2).

The PP/PP-MWCNT composites were prepared by the solution of PP and PP-MWCNTs in *o*-xylene at 150°C . The film and disk of PP/PP-MWCNT composites were fabricated by the hot press (pressure: 5 MPa, temperature: 180°C). The PP/MWCNT composites for

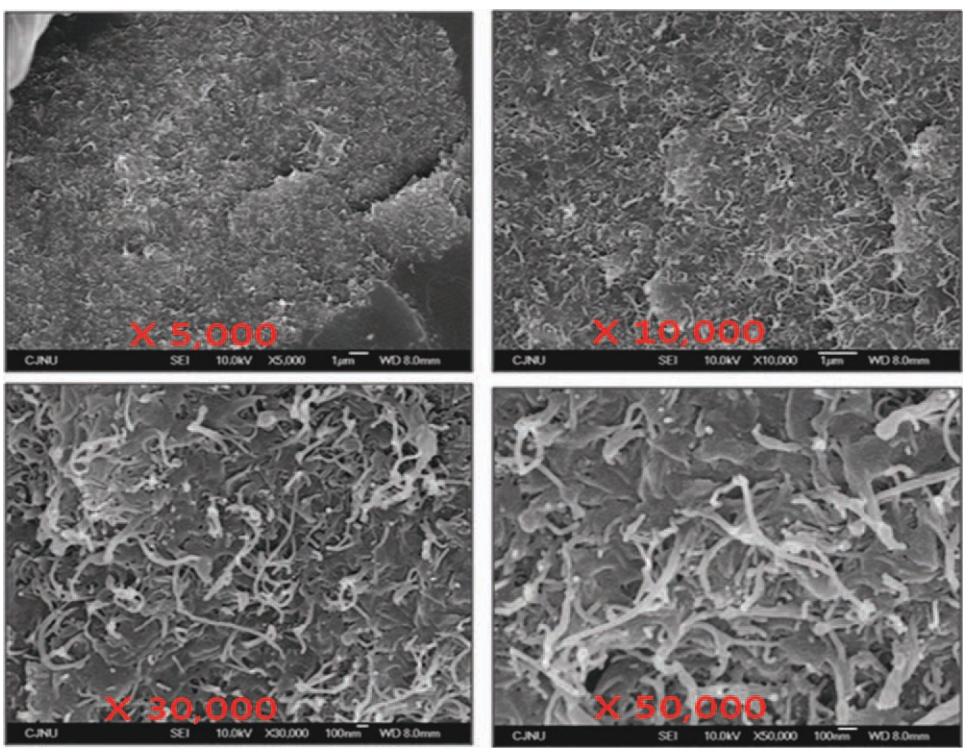

Figure 10 FE-SEM images of cryogenically fractured surfaces of PP/MWCNT composites on Si-wafer. [Color figure can be viewed in the online issue, which is available at wileyonlinelibrary.com.].

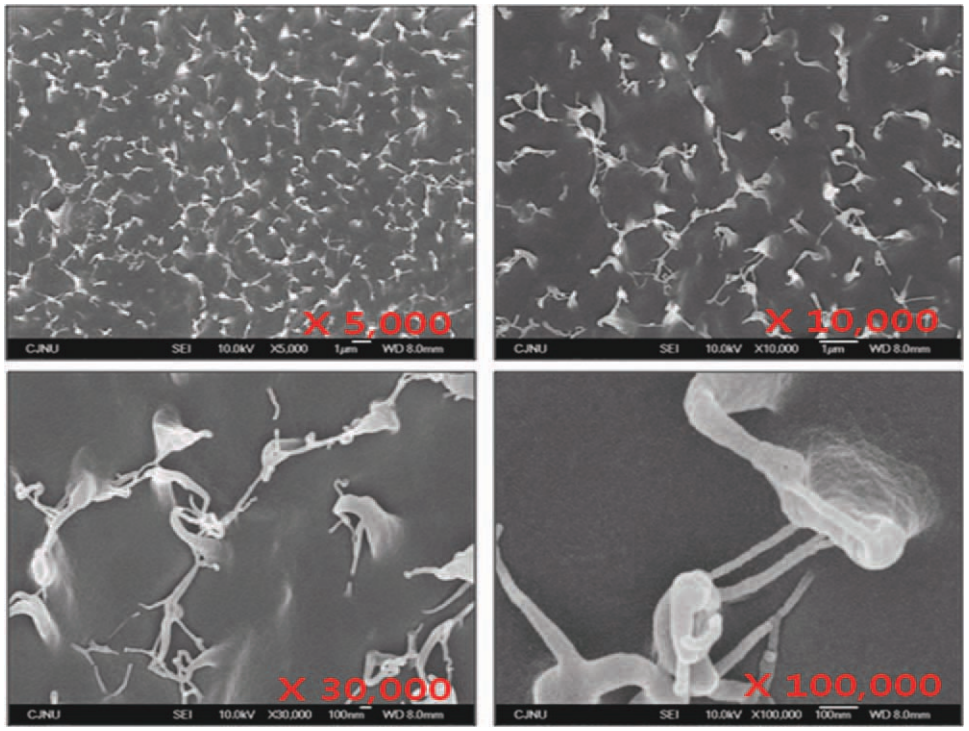

Figure 11 FE-SEM images of cryogenically fractured surfaces of PP/PP-MWCNT composites on Si-wafer. [Color figure can be viewed in the online issue, which is available at wileyonlinelibrary.com.].

the control experiment were prepared by same procedures used in PP/PP-MWCNT composites.

Figure 9 shows the dispersion of MWCNTs and PP-MWCNTs in the PP matrix. For each experiment, the concentration of MWCNTs and PP-MWCNTs in the PP matrix were 1 wt %. As illustrated in Figure 9(a), the both of film and disk of the pure PP exhibit transparency. However, after inclusion with MWCNTs, the PP composites with MWCNTs lost their transparency. Especially, for PP/MWCNT composite containing MWCNTs, severely aggregated masses of MWCNTs are frequently observed on the morphology as seen in Figure 9(b), whereas in the case of PP/PP-MWCNT composites, PP-MWCNTs are spatially well-dispersed in the PP matrix as shown in Figure 9(c). MWCNTs were easily aggregated each other because there is no interaction between PP and MWCNTs. The homogeneous dispersion of PP-MWCNTs is ascribed to the good miscibility of PP and PP-MWCNTs.

The much improved dispersion of PP-MWCNTs in the PP matrix well corresponds to the result investigated by SEM microphotographs of cryogenically fractured surface of PP/MWCNT composites and PP/PP-MWCNT composites as shown in Figures 10 and 11, respectively. MWCNTs were lumped in the PP matrix as shown in Figure 10, whereas PP-MWCNTs were nicely, homogeneously dispersed in the PP matrix through good miscibility of PP and PP-MWCNTs as shown in Figure 11.

To compare the thermal stability of PP, PP/MWCNT composites, and PP/PP-MWCNT composites, thermal analysis was carried out by TGA measurements in an inert atmosphere at a heating rate of 10°C/min as shown in Figure 12. The PP exhibited the initial decomposition temperature at 319°C and was completely decomposed in the temperature around 427°C. However, after inclusion of MWCNTs, the decomposition temperature of

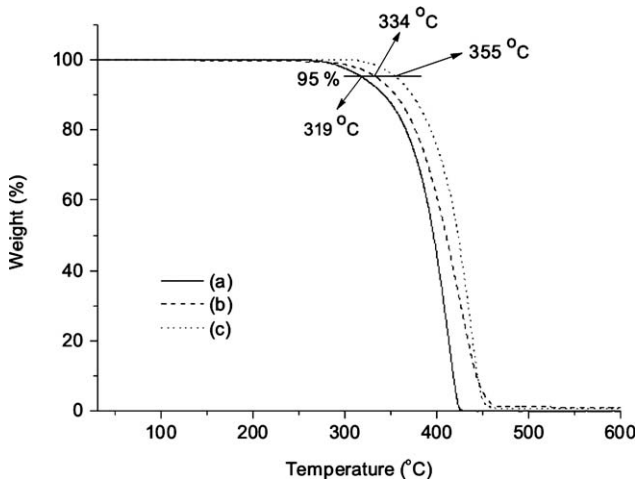

Figure 12 TGA thermograms of (a) PP, (b) PP/MWCNT composites, and (c) PP/PP-MWCNT composites at a heating rate of 10°C/min under nitrogen atmosphere.

TABLE I
Thermal Conductivity and Thermal Diffusivity of PP, PP/MWCNT Composites, and PP/PP-MWCNT Composites

Sample	Thermal diffusivity (cm^2/s)	Density (g/cm^3)	Heat capacity ($J/g\ K^{-1}$)	Thermal conductivity ($W/m\ K^{-1}$)
PP	1.432×10^{-3}	0.831	1.925	0.229
PP/MWCNT composites	2.58×10^{-3}	0.941	1.907	0.464
PP/PP-MWCNT composites	5.27×10^{-3}	0.976	1.83	0.941

hybrid composites with MWCNTs was shifted to a higher temperature than that of PP (319°C). Also, the composites with MWCNTs were not completely decomposed in the temperature range between 450 and 600°C. The reason is that the MWCNTs have good thermal stability. Especially, the PP/PP-MWCNT composites were decomposed at the higher temperature (355°C) than the case of PP/MWCNT composites (334°C). This result shows that the PP-MWCNTs are homogeneously dispersed in the PP matrix.

For the measurement of thermal conductivity of composites, we used the following methods. Thermal diffusivity was measured by laser flash method.[35] Laser heat pulse was irradiated on the front side of sample. The thermal diffusivity was calculated by the increased temperature and time to half of maximum temperature when the heat is transmitted from front side to the back side of sample through the sample thickness.

The specific heat (C_p) values of the composites with MWCNTs were determined by calorimetric measurements using DSC at 22°C. The temperature and heat flow scales were calibrated with indium between 0 and 65°C under nitrogen atmosphere. The following procedure is applied on the empty pan, the sapphire, and the sample inside the pan: annealing for 5 min at 0°C, heating a range from 0 to 65°C at a heating rate of 10°C/min, and annealing for 5 min at 65°C.

Thermal conductivity was calculated from thermal diffusivity with the aid of Eq. (1). In this case, the specific heat and the sample density must be previously known.

$$k = \alpha \rho C_p \tag{1}$$

where k = thermal conductivity ($W/m\ K^{-1}$), α = thermal diffusivity (cm^2/s), ρ = density (g/cm^3), and C_p = specific heat ($J/g\ K^{-1}$). The thermal diffusivity, density, specific heat, and thermal conductivity of composites were measured (Table I).

Figure 13(a) shows the thermal diffusivity of PP, PP/MWCNT composites, and PP/PP-MWCNT composites at 22°C. Thermal diffusivity of PP exhibits the low value up to 0.001432 cm^2/s. However, by adding small amount of MWCNTs, thermal diffusivity was sharply increased by adding 1 wt % of PP-MWCNTs. Thermal diffusivity of PP/PP-MWCNT composites (0.00527 cm^2/s) is larger than that obtained from the PP/MWCNT composites (0.00258 cm^2/s) as shown in Figure 13.

Figure 13(b) shows the thermal conductivity of PP, PP/MWCNT composites, and PP/PP-MWCNT composites. Thermal conductivity of composites in this study was obtained using Eq. (1). Thermal conductivity

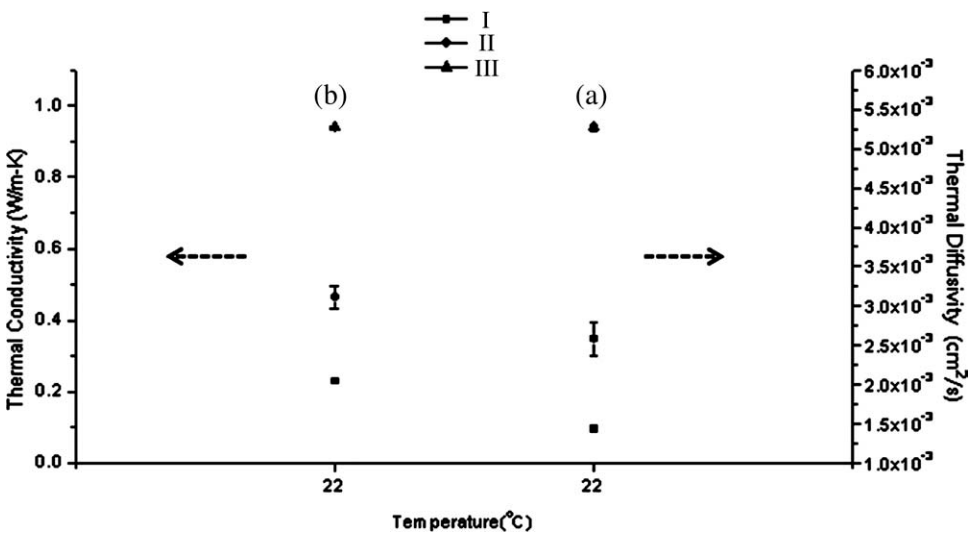

Figure 13 Thermal diffusivity (a) and thermal conductivity (b) curves of composites; (i) PP, (ii) PP/MWCNT composites, and (iii) PP/PP-MWCNT composites at 22°C.

of composites showed the same trend as thermal diffusivity did. The PP, PP/MWCNT composites, and PP/PP-MWCNT composites show the thermal conductivity to 0.229, 0.464, and 0.941 W/m K^{-1}, respectively. Thermal conductivity of PP/MWCNT composites was slightly increased relative to that of the pure PP. To our surprise, thermal conductivity of PP/PP-MWCNT composites was much higher than that of the pure PP and PP/MWNT composites even if only 1 wt % of PP-MWCNTs was added to the PP matrix. This result suggests that PP-MWCNTs are homogeneously dispersed in the PP matrix without any aggregation of PP-MWCNTs. That is, the high miscibility of PP and PP-MWCNTs resulted in the good transparency and the remarkable thermal conductivity. The more detailed regarding the thermal conductivity of PP/PP-MWCNT composites with different contents of PP-MWCNT (0.1, 0.5, 2.0, and 3.0 wt %) will be reported soon in the other literature.

CONCLUSIONS

We have developed a new approach for homogeneous composites of PP and MWCNTs. To overcome the immiscibility between PP and MWCNTs, PP-MWCNTs was fabricated by the reaction of PP-OH and MWNT-Br to make homogeneous PP/PP-MWCNTs composites with higher thermal stability and thermal conductivity than PP/MWCNT composites and the pure PP. From the SEM and TEM images, PP-MWCNTs had PP layers of thickness 10–15 nm on the outer walls of the MWNTs. PP/PP-MWCNT composites were prepared by solution mixing in *o*-xylene. PP-MWCTNs were homogeneously dispersed in the PP matrix through the good miscibility of PP and PP-MWCNTs, which was clearly observed in photograph images and SEM images of cryogenically fractured surface. As a result, the thermal stability of PP/PP-MWCNT composites was improved up to 36°C by TGA measurement as compared to the pure PP. The thermal conductivity of PP/PP-MWCNT composites was increased more than four times relative to that of the pure PP. In addition, the thermal conductivity of PP/PP-MWCNT composites was much higher than that of PP/MWNT composites. It is confirmed that the above enhanced properties are ascribed to the homogeneous dispersion of PP-MWCNTs in the PP matrix by the high miscibility of PP and PP-MWCNTs.

References

1. Wang, C.; Guo, Z. X.; Fu, S.; Wu, W.; Zhu, D. Prog Polym Sci 2004, 29, 1079.
2. Liu, P. Eur Polym J 2005, 41, 2693.
3. Tasis, D.; Tagmatarchis, N.; Bianco, A.; Prato, M. Chem Rev 2006, 106, 1105.
4. Homenick, C. M.; Lawson, G.; Adronov, A. J Macromol Sci Part C Polym Rev 2007 47, 265.
5. Lin, Y.; Meziani, J.; Sun, Y. P. J Mater Chem 2007, 17, 1143.
6. Galli, P.; Vecellio, G. J Polym Sci Part A Polym Chem 2004, 42, 396.
7. Balow, M. J.; Karian, G. H. In Handbook of Polypropylene and Polypropylene Composites; CRC Press: New York, 2003.
8. Velasco-Santos, C.; Martinez-Hernandez, A. L.; Castano, V. M. Compos Interfaces 2005, 11, 567.
9. Moniruzzaman, M.; Winey, K. I. Macromolecules 2006, 39, 5194.
10. Shaffer, M. S. P.; Sandler, J. K. W.; Advani, S. G. In Processing and Properties of Nanocomposites; World Scientific: Singapore, 2007.
11. Schmidt, R. H.; Kinloch, I. A.; Burgess, A. N.; Windle, A. H. Langmuir 2007, 23, 5707.
12. Park, C.; Oundaies, Z.; Watson, K. A.; Crooks, R. E.; Smith, J. J.; Lowther, S. E.; Connell, J. W.; Siochi, E. J.; Harrison, J. S.; Clair, T. L. Chem Phys Lett 2002, 364, 303.
13. Hirsch, A. Angew Chem 2002, 41, 1853.
14. Kim, K. H.; Jo, W. H. Macromolecules 2007, 40, 3708.
15. Lee, J. U.; Huh, J.; Kim, K. H.; Park, C.; Jo, W. H. Carbon 2007, 45, 1051.
16. Wang, M.; Pramoda, K. P.; Goh, S. H. Carbon 2006, 44, 613.
17. Park, S.; Huh, J. O.; Kim, N. G.; Kang, S.; Lee, K. B.; Hong, S. P. Carbon 2008, 46, 706.
18. Xue, C. H.; Zhou, R. J.; Shi, M. M.; Gao, Y.; Wu, G.; Zhang, Z. B. Nanotechnology 2008, 19, 215604.
19. Shanmugharaj, A. M.; Bae, J. H.; Nayak, R. R.; Ryu, S. H. J Polym Sci Part A Polym Chem 2007, 45, 460.
20. Qin, S.; Qin, D.; Ford, W. T.; Resasco, D. E.; Herrera, J. E. J Am Chem Soc 2004, 126, 170.
21. Kong, H.; Gao, C.; Yan, D. J Am Chem Soc 2004, 126, 412.
22. Kong, H.; Gao, C.; Yan, D. Macromolecules 2004, 37, 4022.
23. Qin, S.; Qin, D.; Ford, W. T.; Resasco, D. E.; Herrera, J. E. Macromolecules 2004, 37, 752.
24. Baskaran, D.; Mays, J. W.; Bratcher, M. S. Angew Chem 2004, 43, 2138.
25. Hong, C. Y.; You, Y. Z.; Wu, D. C.; Liu, Y.; Pan, C. Y. Macromolecules 2005, 38, 2606.
26. Liu, Y. L.; Chen, W. H. Macromolecules 2007, 40, 8881.
27. You, Y. Z.; Hong, C. Y.; Pan, C. Y. Nanotechnology 2006, 17, 2350.
28. Hong, C. Y.; You, Y. Z.; Pan, C. Y. Polymer 2006, 47, 4300.
29. Zhao, B.; Hu, H.; Yu, A.; Perea, D.; Haddon, R. C. J Am Chem Soc 2005, 127, 8197.
30. Li, H.; Cheng, F.; Duft, A. M.; Adronov, A. J Am Chem Soc 2005, 127, 14518.
31. Hill, D.; Lin, Y.; Qu, L.; Kitaygorodskiy, A.; Connell, J. W.; Allard, L. F. Macromolecules 2005, 38, 7670.
32. Wang, W.; Lin, Y.; Sun, Y. P. Polymer 2005, 46, 8634.
33. Jeon, J. H.; Lim, J. H.; Kim, K. M. Polymer 2009, 50, 4488.
34. Kaneko, H.; Junji, S.; Nobuo, K.; Shingo, M.; Tomoaki, M.; Norio, K. Polymer 2008, 49, 4576.
35. Parker, W. J.; Jenkins, R. J.; Butter, C. P.; Abbot, G. L. J Appl Phys 1961, 32, 1679.